Structural basis of rhodopsin/G protein coupling : biochemical activity of peptide complexes, photo cross-linking, and mass spectrometric analysis

by Paul Camille Kraft

A dissertation submitted in partial fulfillment of the requirements for the degree Of Doctor of Philosophy In Biochemistry
Montana State University

Abstract:
Physiological and sensory mechanisms are primarily controlled by membrane impermeant signals—which are usually detected by membrane-spanning receptor proteins that ultimately trigger intracellular responses. Similarly, development and repair in multi-cellular organisms are controlled by specific adhesion mechanisms that recognize macromolecular binding sites outside cells and control cytoplasmic responses. Understanding of signaling and adhesion mechanisms could be greatly advanced if the structures of the membrane-spanning receptor proteins and their non-covalent interaction partners could be determined at atomic resolution—but these structures can not typically be deduced by x-ray crystallography or NMR.

Mass spectrometry is able to mass analyze high molecular weight species, however, non-covalent protein-ligand or protein-protein interactions are disrupted by the non-aqueous conditions used in conventional mass spectrometry. This thesis describes new mass spectrometric methodologies to analyze proteins directly from aqueous solutions, which is an important first step in mass spectrometry of non-covalent protein-ligand complexes. Insight is gained into fundamental mechanisms of laser desorption ionization mass spectrometry from aqueous solutions.

This thesis also describes biochemical and mass spectrometric methods to identify non-covalent interactions between the rhodopsin visual receptor and the G protein, transducin. The contacts between rhodopsin and transducin were studied using synthetic peptides derived from transducin that were characterized by their ability to inhibit rhodopsin catalysis of nucleotide binding by transducin. The peptides were also characterized for their ability to inhibit the homologous formyl peptide receptor's catalysis of nucleotide binding by the Gi protein.

Fluorescent photo-activatable analogs of the most potent peptides were synthesized. Non-covalent rhodopsin-peptide interactions were tested for specificity and covalently stabilized by photo-chemical cross-linking. Rhodopsin-peptide complexes (which are about 42,000 Da) must be cleaved into smaller peptides for mass spectrometric analysis of the amino acid sites cross-linked. Cyanogen bromide cleavage of rhodopsin reduced the size of the hydrophobic fragments to facilitate analysis.

Methods are described for mass spectral analysis of all of the cyanogens bromide fragments of rhodopsin at the picomole level, which is an essential first step in identifying the peptide cross-linking sites in rhodopsin. These results represent significant progress in efforts to define the molecular contacts between rhodopsin and transducin and homologous proteins.

STRUCTURAL BASIS OF RHODOPSIN/G PROTEIN COUPLING: BIOCHEMICAL ACTIVITY OF PEPTIDE COMPLEXES, PHOTO CROSS-LINKING, AND MASS SPECTROMETRIC ANALYSIS

By

Paul Camille Kraft

A dissertation submitted in partial fulfillment of the requirements for the degree

Of

Doctor of Philosophy

In

Biochemistry

MONTANA STATE UNIVERSITY
Bozeman, Montana

April 2001

APPROVAL

Of a dissertation submitted by

Paul Camille Kraft

This dissertation has been read by each member of the dissertation committee and has been found to be satisfactory regarding content, English usage, format, citations, bibliographic style, and consistency, and is ready for submission to the College of Graduate Studies.

Edward A. Dratz _____ (Signature) 4/23/2001 Date

Approved for the Department fo Chemistry and Biochemistry

Paul Grieco _____ (Signature) 4/23/01 Date

Approved for the College of Graduate Studies

Bruce McLeod _____ (Signature) 5-2-01 Date

STATEMENT OF PERMISSION TO USE

In presenting this thesis in partial fulfillment of the requirements for a doctoral degree at Montana State University, I agree that the library shall make it available to the borrowers under the rules of the Library. I further agree that copying of this thesis is allowable only for scholarly purposes, consistent with "fair use" as prescribed in the U.S. Copyright Law. Requests for extensive copying or reproduction of this thesis should be referred to Bell & Howell Information and Learning, 300 North Zeeb Road, Ann Arbor Michigan 48106, to whom I have granted "the exclusive right to reproduce and distribute my thesis in and from microform along with the non-exclusive right to reproduce and distribute my abstract in any format in whole or in part".

Signature 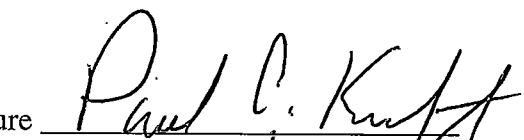

Date 4/23/01

ACKNOWLEDGEMENTS

Thanks to Prof. Edward Dratz, Prof. Jan Sunner, Dr. John Mills, Prof. Sergey Alimpiev, Prof. Heidi Hamm, Dr. Heini Miettinen, Blaine Roberts, and Dr. Joseph Sears.

I would also like to thank my parents, Ken & Anna Kraft, family, friends, and last but certainly not least, Lara Taubner, the love of my life.

TABLE OF CONTENTS

Page

LIST OF TABLES

LIST OF FIGURES

Figure Page

ABSTRACT

Physiological and sensory mechanisms are primarily controlled by membrane impermeant signals—which are usually detected by membrane-spanning receptor proteins that ultimately trigger intracellular responses. Similarly, development and repair in multi-cellular organisms are controlled by specific adhesion mechanisms that recognize macromolecular binding sites outside cells and control cytoplasmic responses. Understanding of signaling and adhesion mechanisms could be greatly advanced if the structures of the membrane-spanning receptor proteins and their non-covalent interaction partners could be determined at atomic resolution—but these structures can not typically be deduced by x-ray crystallography or NMR.

Mass spectrometry is able to mass analyze high molecular weight species, however, non-covalent protein-ligand or protein-protein interactions are disrupted by the non-aqueous conditions used in conventional mass spectrometry. This thesis describes new mass spectrometric methodologies to analyze proteins directly from aqueous solutions, which is an important first step in mass spectrometry of non-covalent protein-ligand complexes. Insight is gained into fundamental mechanisms of laser desorption ionization mass spectrometry from aqueous solutions.

This thesis also describes biochemical and mass spectrometric methods to identify non-covalent interactions between the rhodopsin visual receptor and the G protein, transducin. The contacts between rhodopsin and transducin were studied using synthetic peptides derived from transducin that were characterized by their ability to inhibit rhodopsin catalysis of nucleotide binding by transducin. The peptides were also characterized for their ability to inhibit the homologous formyl peptide receptor's catalysis of nucleotide binding by the Gi protein.

Fluorescent photo-activatable analogs of the most potent peptides were synthesized. Non-covalent rhodopsin-peptide interactions were tested for specificity and covalently stabilized by photo-chemical cross-linking. Rhodopsin-peptide complexes (which are about 42,000 Da) must be cleaved into smaller peptides for mass spectrometric analysis of the amino acid sites cross-linked. Cyanogen bromide cleavage of rhodopsin reduced the size of the hydrophobic fragments to facilitate analysis. Methods are described for mass spectral analysis of all of the cyanogens bromide fragments of rhodopsin at the picomole level, which is an essential first step in identifying the peptide cross-linking sites in rhodopsin. These results represent significant progress in efforts to define the molecular contacts between rhodopsin and transducin and homologous proteins.

CHAPTER 1

INFRARED LASER DESORPTION IONIZATION MASS SPECTROMETRY ON FROZEN AQUEOUS SOLUTIONS OF PROTEINS AND PEPTIDES

Abstract

Surface-assisted, laser desorption ionization (SALDI) time-of-flight mass spectra of proteins and peptides have been obtained from bulk frozen aqueous solutions by adding solid organic powders to the solutions before freezing. Abundant analyte ions were obtained with a 3.28 μm Nd:YAG/OPO laser. Twenty compounds were evaluated as solid additives, and sixteen yielded protein mass spectra. Successful solids included compounds like pyrene, aspartic acid, and polystyrene. The best results were obtained with nicotinic acid and indole-2-carboxylic acid, which yielded protein mass spectra anywhere on the sample and with every laser shot. Compared with UV-MALDI on the same instrument, cryo-IR-SALDI had a comparable detection limit (≈ 1 μM), a lower mass resolution for peptides, and a higher mass resolution for large proteins. Approximately 2,500 cryo-IR-SALDI mass spectra were obtained from a single spot on a 0.3 mm thick frozen sample before the metal surface was reached. About 0.1 nL of frozen solution was desorbed per laser shot. The extent of protein charging varied between the SALDI solids used. With thymine, myoglobin charge states up to MH_{12}^{+12} were observed. It is tentatively concluded that observed ions are pre-formed in the frozen sample.

Introduction

Matrix-assisted laser desorption ionization mass spectrometry (MALDI-MS) is a powerful and widely used method for the analysis of large biochemical molecules [1,2]. In MALDI, the biomolecules are entrained into crystals of a UV-absorbing matrix by solvent evaporation [3]. Irradiation of the sample with a short pulse from a UV laser results in the desorption and ionization of the biomolecules. Together with electrospray [4], MALDI has revolutionized biochemical mass spectrometry.

The goal of performing laser desorption mass spectrometry of biomolecules directly from water solutions has been pursued over several years for a number of reasons. 1) Aqueous solutions constitute the native environment for most biomolecules, and analysis of biomolecules directly from aqueous solutions would require a minimum of sample manipulations. 2) A sample preparation method that uses a water matrix might work equally well for a wide range of biomolecules. Presently, a number of different matrices are used in MALDI, and finding the best matrix and sample preparation method for a given analyte is partly a matter of trial and error. 3) UV-MALDI is sometimes troubled with a wide range of sensitivities for components in mixtures and widely varying signal intensities at different spots on the sample surface. A desorption method with a more uniform and predictable sensitivity would be extremely useful. 4) An aqueous environment is usually necessary to maintain the structure of, and interactions between, most proteins and other biomolecules (although aqueous glycerol is a fairly mild solvent.) Thus, mass spectra of macromolecules in conformations competent to form native intermolecular complexes, as well as the intact

complexes of these molecules, are best obtained directly from aqueous solutions. In MALDI, analytes are subjected to drying in concentrated, usually acidic, organic matrix solutions and to the formation of matrix crystals. During this process, there will be a strong tendency for most biomolecules to denature, and this may well explain why the dissociated subunits of complex proteins are typically seen in MALDI mass spectra. Suitable freezing protocols are able to maintain the native, functional conformation of most protein systems [5,6]. Progress in desorbing macromolecules from frozen aqueous solutions may lead to methods for the reliable and sensitive detection of intact subunit proteins and other non-covalent complexes by laser desorption mass spectrometry. 5) If laser desorption could be performed directly from frozen aqueous solutions, the localized *in situ* detection of proteins and other biomolecules from intact frozen cells and tissues might become possible.

Considering the perceived desirable desorption properties above, it is unfortunate that it has proven to be extremely difficult to obtain gas-phase ions of biomolecules by laser desorption from frozen water ice solutions [7,8]. This situation also represents a challenge to our understanding of desorption/ionization processes.

Presently, UV lasers are almost exclusively used for MALDI mass spectrometry. Nitrogen lasers at 337 nm and Nd:YAG laser harmonics at 266 or 355 nm are common. Water, glycerol, and most organic solvents do not absorb at these wavelengths. However, water and other hydroxylated solvents have strong absorption bands in the IR, near 3 μm [9]. A number of publications have appeared that deal with IR laser desorption mass spectrometry [10-16] and with laser desorption from water and hydroxylated solvents [10,17]. Glycerol

was used as a matrix in the early work by Tanaka et al. [17] who obtained protein mass spectra by using 300 Å diameter cobalt particles to couple the laser energy into the liquid.

Hillenkamp et al. demonstrated IR-MALDI using a 2.94 μm Q-switched Er:YAG laser with a 150 ns pulse width [10]. Protein mass spectra were obtained from several MALDI matrices. However, a spectrum of lysozyme (14 kDa) using a liquid glycerol matrix was also reported [10]. The authors later obtained very similar results when using a pulsed 10.6 μm CO_2 laser [11]. In a recent paper, Hillenkamp et al. reported mass spectra of a range of proteins using glycerol as the matrix [15]. IR-MALDI was reported to have a higher upper mass limit and a higher mass resolution for large proteins than UV-MALDI on the same samples [12,15,18]. Metastable fragmentation of larger proteins, above about 20 kDa, was found to much less of a problem with IR-MALDI [15]. On the other hand, IR-MALDI consumed much more material than UV-MALDI, and only a few spectra could be obtained from the same spot on the desorption probe in IR-MALDI [11,13,15]. This was explained by a large neutral yield with an ablation depth of 0.1 to 0.5 μm in the thin, dry samples employed. Biemann et al. have also demonstrated applications of IR-MALDI to dry samples [19,20], and the application of a Cr:LiSAF pumped OPO laser to IR-MALDI was recently demonstrated [21].

The characteristics of liquid water ablation, induced by high fluence IR laser pulses have been studied (see [22] and references therein). Several factors, including changes in the absorption coefficient of water during the laser pulse [23], the development of shock waves, and delayed ablation have been shown to be important to the dynamics of laser-induced

ablation of water and biological materials with a high water content [22,24]. Of particular relevance to the present work are previous reports of laser desorption of biomolecules, with and without mass spectrometry, from frozen aqueous solutions. Williams et al. reported successful desorption of nucleic acid oligomers by laser ablation from films of frozen aqueous solutions where the water content had been reduced by sublimation in vacuum, such that the film had a total thickness of a few micrometers [7,25-27]. A visible wavelength laser beam from a tunable dye laser heated the underlying copper substrate surface. The reproducibility of ionization was, however, reported to be a problem in these experiments [27,28]. Becker et al. have demonstrated advantages of adding photoabsorbing substituted phenols to frozen films containing DNA [29].

Recently, Hillenkamp et al. demonstrated IR-MALDI mass spectra of proteins from air-dried films of protein solutions. In order to retain residual water in the films, they were frozen before being introduced into the vacuum [8]. An Er:YAG laser (2.94 μm, 150 ns pulse length) was used for these experiments. A mass spectrum was obtained only with the first laser shot, from any one single sample spot. Protein spectra had a rather high mass resolution, in the 300 to 350 range. The upper mass limit was reported to be 30 kDa, with a higher mass limit of 70 kDa if TrisHCl, a known IR MALDI matrix, was added to the aqueous solution [8]. Protein spectra were also reported from a hen egg lysozyme crystal. The authors emphasized that no protein spectra had been obtained from the bulk frozen, aqueous solutions, despite extensive efforts to vary experimental conditions [8].

Alimpiev at al. have used CO_2 lasers for ablation of frozen aqueous solutions. They used a tunable UV laser to ionize desorbed organic molecules by time-delayed, resonance-enhanced, multi-photon post-ionization [30-32]. The method was successful for ultra-high sensitivity detection of simple organic molecules, such as aromatic amino acids and phenol, dissolved in water. However, the upper mass limit of the method was found to be low and was limited by fragmentation of the analyte molecules by the UV and IR lasers.

Recently, we introduced the use of carbon powder suspensions in liquid glycerol as a matrix for laser desorption ionization at room temperature [33], and we refer to this method as Surface-Assisted Laser Desorption Ionization (SALDI) Mass Spectrometry. Graphite SALDI/MS has been applied also to frozen water solutions, as reported at a recent conference [34]. Using the 3.28 μm Nd:YAG/OPO laser, we found that spectra of organic molecules and peptides were easily and reliably obtained. However, with carbon powders we were not successful in obtaining mass spectra of proteins larger than about 20,000 Da. In the present work, we present a SALDI method that uses suspensions of organic crystals, instead of the carbon powder, in frozen, aqueous solutions for cryo-IR-SALDI. This cryo-IR-SALDI MS method reliably produces intense peptide and protein ion signals.

Experimental

Experiments were performed on a modified VESTEC 2000, 1.35 m linear time-of-flight mass spectrometer (Perceptive Biosystems, Framingham, MA). The acceleration voltage was 20,000 V, and all spectra were obtained in positive ion mode. A guide-wire

along the center of the flight tube was suspended from a point 6" from the beginning of the field-free region to a point 2" in front of the ion detector. The guide wire was normally held at -120 V. Unless otherwise noted, the guide wire was used as a low mass gate by switching the guide-wire voltage to +120 V for 3.0 μs after the laser pulse. Time-of-flight mass spectra were recorded on a Tektronix TDS520 storage oscilloscope and downloaded onto a PC for analysis. Internal mass calibration was used.

The tip of a 1/4" stainless steel insertion probe consisted of a copper rod with a 5.0 mm diameter front sample loading surface. This surface was flush with the "sample electrode" surface during desorption. The insertion probe tip made both thermal and electrical contact with the sample electrode plate, and both were maintained at the full acceleration voltage. Two additional electrodes defined the extraction electric field. The first acceleration electrode had a 1/4" central hole, was positioned 0.5" from the sample electrode, and was maintained at half the full acceleration voltage. A second acceleration electrode had a 1/4" central hole covered with a fine wire mesh, was positioned 1.0" from the sample electrode, and was kept at ground potential. With a 20,000 V acceleration voltage, the ion extraction field was 7.9×10^3 V/cm.

The sample electrode was cooled by means of a cold-finger. An electrically insulating BeO ceramic rod was attached to the sample plate. BeO was used because its heat conductivity at low temperature is significantly higher than that of other common electrical insulators [35]. A copper rod was soldered to a stainless steel vacuum feedthrough. Inside the vacuum chamber, the copper rod was connected to a copper holder of the BeO rod by

means of a flexible, braided copper strap. Outside the vacuum chamber, the copper rod dipped into a liquid-nitrogen-filled Dewar. One end of a 1/4" diameter aluminum garnet rod was also attached to the sample electrode, and a thermocouple was glued to the other end with epoxy. The temperature of the electrode was monitored with a Fluke 52 digital thermometer (John Fluke, Palantine, IL). Approximately 45 minutes after filling the Dewar with liquid nitrogen, the sample electrode temperature stabilized at about -140°C. A TV camera (Watec 902, Edmund Scientific) was aimed through a view-port at the top of the ion source chamber, and the sample surface was viewed with 19x magnification on a TV monitor.

The mass spectrometer was equipped with a Nd:YAG/OPO IR laser with a fixed wavelength of 3.28 μm (Big Sky Laser, Bozeman, MT). A maximum of about 200 mJ of a 1.064 μm laser pulse from the Nd:YAG laser (model CFR 400) was used to pump a double-pass, KTP OPO crystal. The crystal was used in a non-critically phase matched condition (90° phase matching) to give a signal beam at 1.57 μm and an idler beam at 3.28 μm. A dichroic mirror was used to reflect the signal beam out of the idler beam path. The 3.28 μm IR beam had a pulse length of 6 ns, and the divergence of the beam was 26 mrad (86.5% energy content) as determined by a central fraction method (energy through an aperture) in the far field. The pulse energy was monitored by a calorimeter (Scientech MA10, Boulder, CO) and was varied from zero to a maximum of 3.5 mJ, by changing the power to the Nd:YAG flash lamps. A nitrogen UV laser (Laser Science Inc., Newton, MA) operating at 337 nm was used for some experiments.

The IR beam was focussed onto the probe tip using a 180 mm focal length CaF_2 lens positioned outside a CaF_2 viewport window. The diameter of the IR laser beam at the lens was 60 mm. The laser beam passed the window normal to the window surface and hit the sample at a 60° angle relative to the normal of the probe surface. The UV beam was focused onto the sample surface in an identical manner, except that the UV beam entered the ion source from the opposite side, through a silica lens and window.

There was a concern that low intensity laser light at 1.57 μm and 1.064 μm, leaking through the dichroic mirror in the IR laser path, might contribute to the desorption process. In control experiments, a Ge-plate that absorbs at both of these wavelengths, but transmits efficiently at 3.28 μm, was inserted into the beam path. No differences in the mass spectra were observed, with or without the Ge-filter, when compared at the same pulse energy.

The focal spot size on the probe tip was measured by the following procedure. When the probe tip was covered with a fine graphite powder, the luminescence of the irradiated area was easy to distinguish on the TV monitor. The focal spot was seen to be ellipsoidal and, by comparing with the known dimensions of the probe tip, it was determined that the irradiated surface area was 0.5 mm^2. Correcting for the 60° incidence angle, the laser beam cross section is found to be 0.25 mm^2. With a typical pulse energy of 3.0 mJ, and correcting for 10% Fresnel losses in the lens and 10% reflection losses in the chamber window, the energy fluence (perpendicular to the laser beam), I_o, is calculated to be 1.0 J/cm^2 and the irradiance 1.9×10^8 W/cm^2 at the focal point. The energy deposition in the sample closest to the surface (at a depth that is small relative to $1/\varepsilon$, where ε is the absorption coefficient) is $\varepsilon \times I_o$, where

I_o is the energy fluence in the laser pulse. The absorption coefficient for water ice at 3.28 μm is approximately 2.5 x 10^3 cm^{-1} [9]. For frozen glycerol, we have measured an absorption coefficient of 1.5 x 10^3 cm^{-1}. Assuming an actual absorption coefficient in our samples is 2 x 10^3 cm^{-1}, we find that energy is deposited in the outermost surface layer with a density of 2 x 10^3 J/cm^3. The energy absorbed may be further lowered by reflection losses in the sample surface and by a decrease in the water absorption coefficient, at 3.28 μm, during irradiation [22].

The liquid solvent consisted of water and glycerol (33:67 w/w), unless otherwise noted. This is the eutectic composition of water and glycerol, and the mixture is thermodynamically stable as a liquid to -46°C [36]. Proteins or peptide analytes were dissolved directly into the solvent at room temperature at concentrations from 0.5 μM to 1 mM. The sample probe tip was cleaned with ethanol, and about four microliters of analyte solution in glycerol/water were typically deposited on the probe surface. A small amount of solid powder was placed on the liquid surface using a spatula, and after a few seconds, any excess dry powder was blown off the sample. Some solid powders like nicotinic acid had good wetting properties and quickly formed evenly distributed suspensions. Other powders with poor wetting properties, like polystyrene, tended to remain on the liquid surface. In those cases, suspensions were formed on the probe tip by stirring the powder into the solvent with a spatula for up to one minute. Sufficient powder was added to give the suspension a slurry-like appearance. After stirring, the surface of the slurry was seen to gradually become smooth, but this process was relatively slow. If too much solid powder was added, the

fluidity of the suspension was lost, and inferior mass spectra were obtained. If too little powder was added, reproducibility suffered and ion intensities decreased. For nicotinic acid, between 0.3 mg and 0.5 mg powder was added per 1 μL solvent. All chemicals used in this work were obtained commercially.

Samples of bacteriorhodopsin were prepared by adding 4 μL of 2-pentanol to 4 μL of a suspension of purple membranes in the glycerol/water solvent. The nicotinic acid crystals were then added, and the suspension was observed to turn yellow. The yellow color indicated that the protein partially denatured in the presence of the nicotinic acid crystals, possibly because the pH decreased to 3.5.

After preparing a suspension, the probe tip was cooled by immersion into liquid nitrogen. With the eutectic glycerol/water mixture, this cooling resulted in the formation of a vitreous phase, with essentially no ice crystal formation [37]. Immersion of the sample into liquid propane resulted in much faster cooling, but did not change the mass spectra when the glycerol/water eutectic mixture was used. A thin water frost layer was formed on the cold sample surface as the probe was transferred from the Dewar, where it was frozen, to the vacuum lock of the mass spectrometer. Using a 1 Hz laser repetition rate to obtain single shot mass spectra on the oscilloscope, it was found that weak protein ion peaks were observed from the first laser shots. The protein peaks gradually approached their full intensity during the first 50 laser shots at 3 mJ.

To avoid the formation of a frost layer, the room temperature probe tip with the eutectic glycerol/water sample solution could be inserted into the ion source. The sample was

then cooled *in situ* upon contact with the pre-cooled sample electrode. The cooling was still fast enough (about 1 minute to reach -130°C) that the eutectic solution formed a vitreous phase [37]. The protein mass spectra obtained with in-situ cooling were indistinguishable from the ones obtained by fast cooling in liquid nitrogen (after ablation of the frost layer). However, all spectra shown in this paper were obtained by immersion of the sample in liquid nitrogen. Cooling below -100°C did not significantly change the mass spectra. All spectra were obtained at -140±5°C, unless otherwise noted.

About half of the compounds tested in this work as cryo-IR-SALDI solids had a low or negligible solubility in glycerol/water. However, other solids used, such as nicotinic acid and the amino acids, had a significant solubility. If all the added crystals dissolved fully, no mass spectra were obtained from the bulk of the frozen solutions. Some solids, in particular aspartic acid and histidine, dissolved quickly. Additional powder typically had to be added to ensure that some crystals remained. The dissolution of the soluble solids could be arrested by quickly freezing the sample. Essentially no additional dissolution was observed once the suspensions had been cooled to below -40°C. However, fast freezing also tended to result in an uneven distribution of solid particles in the suspension, and this made it more difficult to obtain high quality mass spectra. A better alternative was to slow the rate of dissolution by pre-cooling the probe and the liquid sample solution to about 0 °C prior to adding the soluble powder. There was then enough time to distribute the solid evenly throughout the suspension.

Control experiments were performed in which either the organic solid or the glycerol was eliminated from the sample. In the absence of organic solids, mass spectra (of peptides) were only occasionally obtained from the bulk of the frozen phase, and these rare events may well have been due to contamination of the sample by solid particles. In experiments where the glycerol cryoprotectant was not present, it was necessary to freeze the sample prior to inserting the probe into the ion source because the high vapor pressure of water near room temperature led to severe loss of the water solvent in the vacuum. Mass spectra were obtained in the absence of glycerol, as described in the Results and Discussion section.

It is well known that laser desorption mass spectra can be obtained from metal surfaces [8,25,28]. For this work, it was necessary to verify that the mass spectra were obtained from the bulk of the frozen suspensions without involvement of the underlying metal surface. "Laser drilling" experiments were performed where 4 μL of the glycerol/water nicotinic acid suspension was first deposited on the probe, and series of laser pulses were delivered to the same spot close to the center of the sample where the sample thickness was approximately 0.30 mm. The copper surface was reached after about 2,500 laser pulses (about 4 minutes at 10 Hz) with a 3 mJ laser pulse energy. That the copper surface was indeed reached at this point was clearly revealed by bursts of intense ion signals due to Na^+, K^+, and Cu^+ that were not seen from the bulk suspension. Thus, the ablation yield was approximately 0.1 μm per 3.0 mJ laser pulse, and the volume of frozen solution desorbed per laser shot was less than 0.1 nL. Unless otherwise noted, the sample size used in this work was 4 μL, the laser was focussed close to the center of the frozen sample, and all spectra

reported were obtained prior to 2 minutes irradiation time (at each spot) at 10 Hz. Under these conditions, the maximum depth of ablation should be less than 25% of the sample thickness.

Results and Discussion

The goal of this work was to obtain mass spectra of biomolecules directly from bulk frozen aqueous solutions. In initial experiments, no solid crystals were added to the analyte solutions in glycerol/water. It was found that the Nd:YAG/OPO laser beam at 3.28 μm was efficiently absorbed by frozen water and glycerol/water solutions, and sample drilling experiments showed that the ablation yield was about 0.3 μm per 3 mJ laser shot [38]. However, we had little success in obtaining mass spectra from the bulk of frozen water or glycerol/water solutions, although peptide mass spectra were occasionally obtained [38]. This is in general agreement with results of Williams et al. [26,27,39] and Hillenkamp et al. [8].

Because useful analyte mass spectra were not obtained from bulk, frozen aqueous solutions, we explored the use of Surface-Assisted Laser Desorption Ionization (SALDI) mass spectrometry [33] to obtain spectra from frozen water solutions. Suspensions of graphite (or activated carbon) particles in aqueous solutions were frozen and irradiated with the 3.28 μm Nd:YAG/OPO laser. It was found that mass spectra of organic molecules and peptides were easily and reliably obtained [34]; however, we were not successful in obtaining mass spectra of proteins larger than myoglobin. In an effort to overcome this limitation, we

explored the use of organic crystals, instead of carbon powder, for cryo-IR-SALDI in frozen, aqueous solutions.

Cryo-IR-SALDI mass spectra of peptides

We first present typical cryo-IR-SALDI results for peptides, before discussing results for proteins. For the mass spectrum of angiotensin II in Figure 1, a suspension of nicotinic acid crystals was prepared and frozen as described in the Experimental section. It is seen that the mass spectrum is dominated by the protonated peptide peak at m/z=1047 and by peaks due to the SALDI solid. Low-intensity clusters of glycerol with Na^+ and K^+ are also sometimes observed.

The mass resolution, ($m/\Delta m$, FWHM), for the peptide peak in Figure 1 is approximately 80. The intensity of the angiotensin peak is low relative to the matrix peaks in the spectrum in Figure 1. This spectrum was obtained at a 1.25 mJ laser pulse energy, and the intensity of the peptide peak was found to increase by about a factor of 10 when the laser pulse energy was increased to the maximum of 3.5 mJ. However, the mass resolution decreased somewhat at higher laser pulse energies. By decreasing the pulse energy below 1 mJ, a mass resolution of 250 (FWHM) could be achieved. This is similar to the mass resolution obtained with UV-MALDI on the same instrument. Using the maximum laser pulse energy, the detection limit (S/N = 3) for angiotensin II was approximately 0.5 μM, or 0.5 pmole for a 1 μL sample.

A 0.5 μM detection limit corresponds to 0.5 pmole of peptide in a 1 μL sample size. However, it is easy to use smaller sample sizes. In room temperature, activated carbon-UV-SALDI, we found that the minimum amount of analyte required was lowered by more than two orders of magnitude by introducing a solvent concentration step on the probe (similar to solvent evaporation in MALDI) and by using smaller sample sizes. These strategies should be possible to use also in cryo-IR-SALDI. The peptide sample consumption during the 100 laser shots used for the spectrum in Figure 2 was about 10 pmole. However, single shot mass spectra were obtained with a peptide consumption of approximately 1 fmole.

Figure 2 shows the abundance of protonated nicotinic acid and protonated angiotensin II, as a function of laser pulse energy in a double logarithmic plot. As the laser pulse energy is increased, the ratio of the abundances of these two ions remains nearly constant up to 1.5 mJ pulse energy, after which the peptide ion abundance is seen to level off more quickly than that of protonated nicotinic acid. The slope of the straight lines at lower laser pulse energy in Figure 2 is approximately 9 for both the nicotinic acid and the peptide which shows that the ion yields increase as the 9th power of the laser pulse energy. This is similar to the slope observed for matrix ions in MALDI [40]. The amount of nicotinic acid in the sample used for Figure 2 was approximately 3,600 times the amount of the peptide, whereas the signal abundance ratio is seen to be about 20. Thus, the relative response for the peptide is much higher than for the SALDI solid.

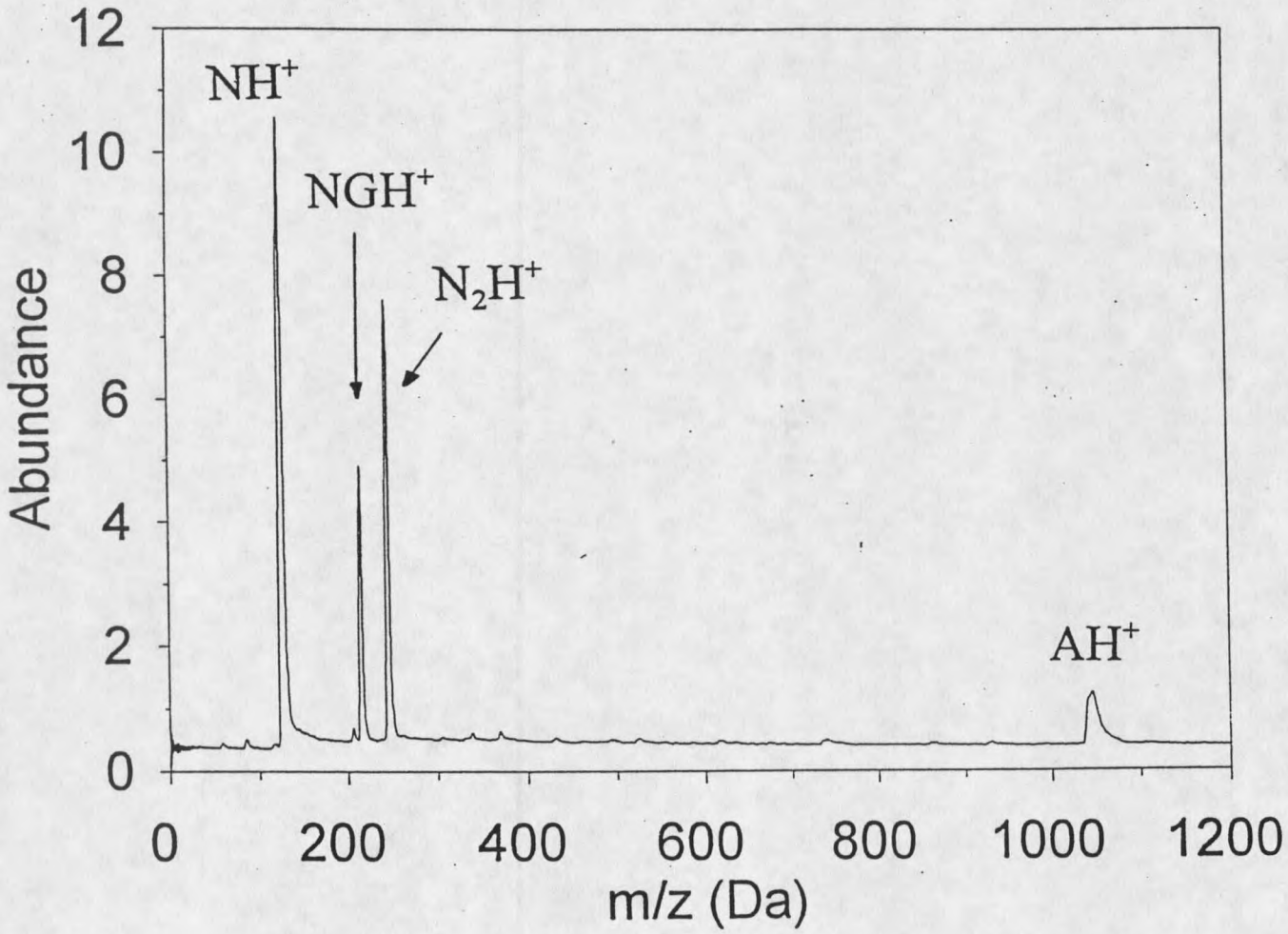

Figure 1. Cryo-IR-SALDI mass spectrum of 0.9 mM angiotensin II in 67% glycerol in water. Nicotinic acid (1.6 mg) was added to 4 μL of the glycerol/ water solution before freezing by immersion of the copper sample tip in liquid nitrogen. Laser pulse energy 1.25 mJ, average of 100 single shot spectra, and low mass gate off. "N" = nicotinic acid, "A" = angiotensin II, and "G" = glycerol.

Comparison between different SALDI solids for protein desorption

We evaluated 20 different organic compounds as SALDI solids using a 0.5 mM equimolar mixture of myoglobin and cytochrome c in the eutectic glycerol/water solution, and the results are summarized in Table 1. Starting at the top of Table 1, the solids evaluated are ordered from the "best" to the "worst" SALDI solids. The approximate signal intensities for the protein peaks are given in the Table, as well as comments on sample preparation. With practice, protein mass spectra were obtained with 16 of the 20 solids. We were unsuccessful with only four of the compounds tested: sodium chloride, cellulose, carboxy-methyl cellulose, and tryptophan. Figure 3 shows a selection of cryo-IR-SALDI protein mass spectra, obtained using (a) nicotinic acid, (b) histidine, © xanthine, and (d) polystyrene as the SALDI solids. The spectra illustrate similarities and differences observed among cryo-IR-SALDI mass spectra using different solids. Singly and multiply charged protein peaks dominate the mass spectra. Several protein/heme and protein/protein clusters, with masses up to 50,000 Da, are resolved in the nicotinic acid and histidine-assisted mass spectra. The extent of multiple charging, and of clustering, is seen to vary between the SALDI solids.

The majority of SALDI solids tested were aromatic compounds, see Table 1. Aromaticity may well contribute to a compound being a successful SALDI solid, but it is not an absolute requirement. For example, aspartic acid crystals gave cryo-IR-SALDI mass spectra of myoglobin and cytochrome c, though the spectra were of lower quality (results not shown). Also, SALDI solids do not have to be volatile or have a low molecular

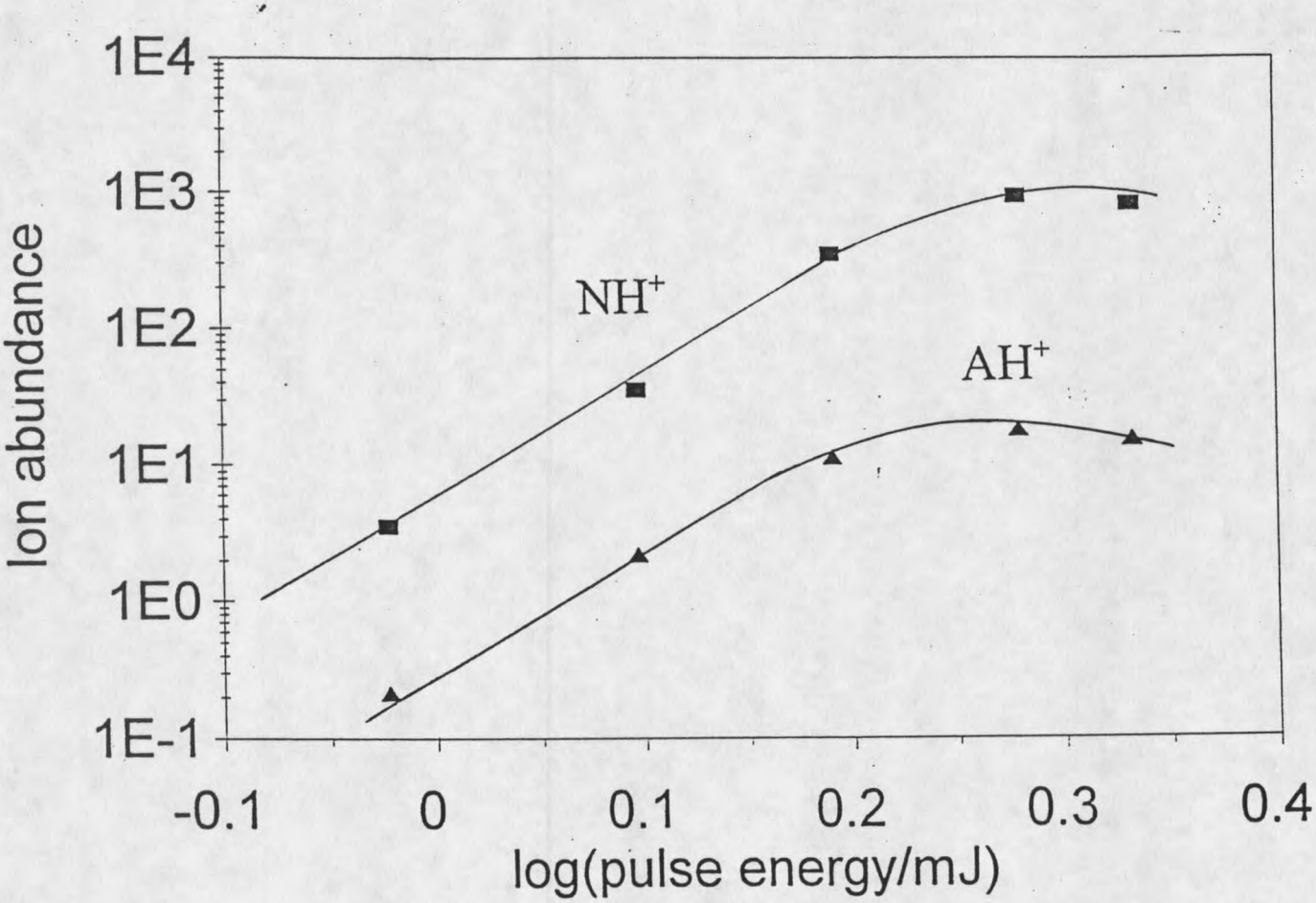

Figure 2 Abundances, as determined by peak heights, of singly protonated nicotinic acid (NH^+) and singly protonated angiotensin II (AH^+) ions as a function of laser pulse energy using the same experimental conditions as in Figure 1.

weight, as illustrated by the fact that polystyrene gave cryo-IR-SALDI mass spectra of proteins, Figure 3d.

The best protein mass spectra with respect to sensitivity and mass resolution were obtained with nicotinic acid, indole-2-carboxylic acid, thymine, and histidine. The mass resolution, m/Δm (FWHM), of the singly charged protein peaks at 15-20 kDa was typically about 50, with somewhat higher resolution obtained at the lowest laser pulse energies. The limit of detection for myoglobin and cytochrome c was about 5-10 μM, compared to about 0.5 μM for peptides, at a signal-to-noise ratio of three. The higher detection limit for proteins as compared to peptides is mainly due to the wider mass peaks for proteins. When peak areas in mass spectra (plotted versus flight time) were compared, it was found that the response for the proteins was close to that for the peptides.

Nicotinic acid was the SALDI solid of choice in this work. Mass resolution and sensitivity were as good as, or better than, those obtained with any of the other solids evaluated. Nicotinic acid, together with indole-2-carboxylic acid, was unique in that it reliably yielded protein mass spectra anywhere on the sample and with every laser shot. In addition, the nicotinic acid powder wets easily, and the suspensions were easy and quick to prepare.

UV-laser irradiation of cryo-SALDI samples

All solids in Table 1 were also tested for their ability to yield cryo-SALDI mass spectra with the 337 nm nitrogen UV laser. In most cases, no ions were observed when the UV laser was first focussed onto a freshly frozen SALDI suspension, but weak signals due

Table 1. Summary of cryo-IR-SALDI results for selected solids additives.

Compound	Protein Mass Spectra Typical Intensity*	Comments
nicotinic acid	5	wets well, fine uniform crystalline powder, rather soluble, low protein charge states
indole-2-carboxylic acid	5	wets well, insoluble, high protein charge, lower mass resolution than nicotinic acid
histidine	4	wets well, very soluble, reliability of analyte signal improved by pre-cooling the glycerol/water solvent before adding crystals
thymine	3-4	poor wetting, required stirring, slightly soluble, dendritic crystals, produces high protein charge states
alpha cyano-4-hydroxy cinnamic acid	2	wets well, almost insoluble, produces high protein charge states
pyrene	1	insoluble, large crystals
6-dimethylaminopurine	1	wets well, slightly soluble
guanine	1	wets well, almost insoluble
xanthine	1	wets well, slightly soluble, tendency to produce high protein charge states
adenine	1	wets well, slightly soluble
2,3-dihydroxybenzoic acid	1	poor wetting, required stirring
sinapinic acid	1	poor wetting, required stirring, insoluble
polystyrene powder (typical m.w. 4,000)	0.5	polystyrene powder was ground by mortar and pestle to remove trapped air, insoluble, required extensive stirring
terepthalic acid	0.5	extensive stirring required, fine powder, insoluble
diphenylamine	0.5	extensive stirring required, large planar crystals do not wet, insoluble
aspartic acid	.5	wets well, very soluble, reliability of analyte signals improved by pre-cooling the glycerol/water solvent before adding crystals
tryptophan	none	slightly soluble
sodium chloride	none	very soluble
cellulose	none	19 μm particle size, wets well, insoluble
carboxy-methyl cellulose	none	insoluble, wets well

*All 20 compounds were tested with a solution of 0.5 mM cytochrome C and 0.5 mM myoglobin in 67% glycerol in water, at ~3.0 mJ per laser shot. Other conditions were as described in the Experimental section. Typical intensities represent the average of one hundred spectra and are quoted in arbitrary units.